GEOCHEMISTRY OF LABORATORY ANOXIC LIMESTONE DRAINS[1]

by

P. Sterner, J. Skousen and J. Donovan[2]

Abstract: An anoxic limestone drain (ALD) is a passive treatment system for treating acid mine drainage (AMD). Historically it has been thought that AMD containing Fe^{3+} and Al^{3+} severely inhibits or stops limestone dissolution due to coating of limestone surfaces by precipitates generated during the neutralization process. Limestone dissolution in field ALDs is difficult to quantify because sampling of the water in ALDs at various locations is not possible, and fluctuations in flow and water chemistry affect limestone dissolution rates. Laboratory experiments were developed to determine the effects of Fe^{3+} and Al^{3+} precipitation on limestone dissolution and the controlling precipitation reactions. Synthetic AMD containing Fe^{3+} or Al^{3+} with and without sulfate was pumped through limestone-packed columns constructed with three sampling ports at equidistant intervals along the column. Water and sediments were periodically extracted for analysis at all sampling ports over a 12-hr period. Results show the majority of limestone dissolution occurred within the first 1.2 hrs of water-limestone contact. Limestone dissolution rate decreased with time and distance along the flow path. Higher concentrations of Fe^{3+} and Al^{3+} (increases in mineral acidity and ionic strength) enhanced limestone dissolution. Geochemical modeling predicted that solutions were nearest equilibrium with respect to the amorphic metal hydroxide phases. Although solutions were periodically oversaturated with respect to sulfate containing minerals, but no x-ray identifiable sulfate minerals were found in the solid phase. The data suggest that smaller anoxic limestone drains may be used when the goal is to neutralize mineral acidity, thus reducing spatial requirements. However, if the goal is to treat AMD to NPDES limits, ALDs may not be a viable long term treatment alternative.

Additional Key Words: acid mine drainage, acid mine drainage treatment, metal precipitation, passive acid mine drainage treatment, saturation indices.

Introduction

One method of treating acid mine drainage (AMD) at abandoned mine sites is by installing anoxic limestone drains (ALDs). An ALD is a buried trench of limestone (kept anaerobic) through which AMD is diverted (Skousen 1991), and it provides a low cost treatment alternative to chemical treatment. The working premise of an ALD is based on limestone dissolution when contacted by anaerobic, low pH water. As the limestone dissolves due to the solution being undersaturated with respect to calcite, the pH rises and the water becomes buffered by bicarbonate (HCO_3^-) alkalinity. Dissolved Fe^{2+} remains in solution as long as the ion is not oxidized. As the water exits the ALD, Fe^{2+} in solution oxidizes, hydrolyzes and precipitates in a sedimentation pond. However, if Fe^{3+} and Al^{3+} are present in water entering an ALD, the pH rise will cause $Fe(OH)_{3(a)}$ and $Al(OH)_{3(a)}$ to precipitate as the solution becomes saturated with respect to these amorphous metal hydroxide phases (denoted by subscript a), thereby compromising the integrity and long term treatment effectiveness of ALDs due to $Fe(OH)_{3(a)}$ and $Al(OH)_{3(a)}$ coating of limestone surface reaction sites. Once these sites are coated, limestone dissolution rate severely decreases or stops, which, in turn, inhibits pH rise, keeps metals in solution, and renders the ALD ineffective.

A few chemical parameters are necessary for successful AMD treatment by ALDs. Turner and McCoy (1990) determined that ALDs function best when dissolved oxygen (DO) is <1 mg L^{-1} because this low oxygen content reduces the amount of Fe^{2+} oxidation that can occur as a result of chemical and chemolithotrophic

[1] 1998 National Meeting of the American Society for Surface Mining and Reclamation, St. Louis, Missouri, May 16-21, 1998.

[2]P. Sterner is Research Assistant and J. Skousen is Professor and Extension Reclamation Specialist in the Division of Plant and Soil Sciences; J. Donovan is Assistant Professor in the Department of Geology; West Virginia University, Morgantown, WV 26506.

Proceedings America Society of Mining and Reclamation, 1998 pp 214-234
DOI: 10.21000/JASMR98010214

https://doi.org/10.21000/JASMR98010214

bacterial oxidation. Skousen et al. (1992) recommended that dissolved Fe^{3+} and Al^{3+} concentration be <25 mg L^{-1}. If these conditions are met, limestone dissolution should continue with minimal coating of limestone or pore clogging by metal hydroxide precipitates.

Acid mine drainage chemistry within ALDs has been monitored at several field sites, but field results have been mixed and are difficult to evaluate. Hedin et al. (1994) determined geochemical parameters of two field sites using mineral saturation indices calculated by the computer equilibrium speciation model WATEQ4F (Ball et al. 1987). The model predicted that no metal hydroxides were precipitating within the drains and that the ALDs should continue to function optimially as long as no drastic changes in influent water chemistry take place. However, Hedin and Watzlaf (1994) demonstrated that ALDs retain metal hydroxides due to hydrolysis and precipitation reactions. Metal hydroxide formation and retention during neutralization in ALDs occurs at pH 3.0 to 4.0 for Fe^{3+} and 4.0 to 5.0 for Al^{3+} (Hedin and Watzlaf 1994).

While field results provide important water quality data and help scientists predict general ALD performance, field studies are unable to accurately quantify the geochemical processes taking place within ALDs for several reasons. Influent chemistry is highly variable, making it difficult to monitor chemical reactions over a sustained time period. Flow rates vary yearly, seasonally, and daily due to climatic changes and precipitation events, which produce differences in water-limestone contact times, water chemistry, and concentration of dissolved solids. Strictly anoxic conditions are difficult to find in near surface environments, and problems encountered during ALD construction sometimes increase dissolved oxygen concentration in the water. Plastic liners used for exclusion of O_2 often rip during construction, allowing O_2 diffusion into AMD. Often, ALDs are not lined, allowing groundwater infiltration into the ALD thereby changing flow and water chemistry, making it difficult to carefully quantify processes that take place within an ALD.

A laboratory setting provides better control of variables and allows an opportunity to quantify the geochemical processes within an ALD. Variation can be controlled by having uniform water chemistry and consistent flow. Sampling along the flow path can also take place in a laboratory setting with less likelihood of introducing air into the ALD. The objectives of this study were to determine the effects of hydroxide precipitation reactions on limestone dissolution and to evaluate the controlling precipitation reactions predicted by the equilibrium speciation model WATEQ4F.

Materials and Methods

Limestone

Limestone of >90% calcium carbonate equivalent was obtained from Greer Limestone (Greer, WV). The limestone was sieved to 1.25 to 1.9 cm (0.5 to 0.75 in) shortest dimension. Upon sieving, the limestone was washed with tapwater to remove dust and loose granular particles. The limestone was air dried and stored until utilized.

Anoxic Limestone Drain Construction

Anoxic limestone drains (Fig. 1) were constructed of 15-cm (6-in) diameter polyvinyl chloride (PVC) pipes. The PVC pipes were cut into 91 cm (36 in) lengths. Three holes were drilled at 23-cm (9-in) intervals to yield three sampling ports. Sampling ports were prepared by extruding a silicone sealant bead around the hole and inserting a flanged rubber vaccine bottle stopper into the hole. A second silicone sealant bead was placed around the stopper to limit gas and liquid exchange. The bottom end of the pipe was fitted and sealed with a PVC cap. A hole was drilled in the cap and fitted with a connector tip, which served as the influent. A weighed amount of limestone was added carefully to the pipe, so as not to disturb the installed sampling ports. The top of the pipe was sealed, drilled, and fitted with a connector tip, which served as the effluent.

Synthetic AMD

Synthetic AMD was prepared and stored in a 50-L polyethylene carboy. The top of the carboy was sealed with a cap containing two outlets. One outlet was fitted with a 76-cm-long (30-in) gas dispersion tube and was used as a sparge line to displace O_2 with Ar. A second outlet had no tubing attached and acted as a vent. The carboy was placed onto a stir plate and filled with 50 L of distilled deionized water (DDW) while being stirred. The water was sparged with Ar until DO concentration was <0.9 mg L^{-1}.

Synthetic AMD was prepared by dissolving the desired amount of chemical salt into 0.5 L of degassed DDW. The dissolved chemical salt was added to the degassed water in the carboy and allowed to mix for at least 5 min prior to experimentation. The experiment commenced by filling the ALD with synthetic AMD from

the bottom. When the AMD exited the top of the tube, pumping began at a rate of 30 ml min^{-1}. The experiment was considered to be at time zero when pumping began and proceeded for 12 hours.

Experimentation

Two experimental modules were devised to complete the research project (Figs. 2 and 3). Module 1 (Fig. 2) consisted of 6 experiments (replicated twice) containing three concentrations each of Fe^{3+} or Al^{3+}, but no sulfate. Module 2 (Fig. 3) consisted of 6 experiments (replicated twice) that contained Fe^{3+} and sulfate or Al^{3+} and sulfate. During the second module, Fe^{3+} and Al^{3+} concentrations were kept static and sulfate was varied to produce 1.00x, 1.25x, and 1.50x the molar concentrations of the acid cation. The chemical salts utilized were $FeCl_3 \cdot 6\ H_2O$, $AlCl_3 \cdot 6\ H_2O$, Na_2SO_4, and H_2SO_4. The salt, Na_2SO_4, was used in conjunction with $AlCl_3 \cdot 6\ H_2O$ for the mixed Al^{3+} and sulfate trials. The acid, H_2SO_4, was used instead of Na_2SO_4 for Fe^{3+} and sulfate experiments because Fe compounds precipitated within the carboy with Na_2SO_4 added.

Water samples were taken at the effluent, and ports 3, 2, and 1 (in this order) at each sampling time (0.25, 0.5, 0.75, 1, 2, 4, 6, 8, 10, and 12 hrs). Samples were taken by inserting 60-ml syringes fitted with hypodermic needles into the sampling ports. Experiments containing Fe^{3+} were passed through 0.45 μm filters (APHA 1992) into 20-ml acidified borosilicate vials. Experiments containing Al^{3+} were passed through 0.1 μm filters into 20-ml acidified borosilicate vials (Roberson and Hem 1967). Samples analyzed for anions were passed through 0.2 μm filters into unacidified 20-ml polyethylene vials. Samples analyzed for acidity and alkalinity by automatic titration (Radiometer America High Performance TitraLab™ High Performance Titration Laboratory) were taken by placing two 10-ml unfiltered aliquots into separate 118-ml containers (APHA 1992).

Samples were analyzed onsite for temperature (°C), pH, electrical conductivity (mmhos cm^{-1}), oxidation-reduction potential (mV), and dissolved oxygen (mg L^{-1}). Alkalinity and acidity were determined by titrating to pH endpoints of 4.2 and 8.3, respectively. Cations were measured by three analytical instruments. Calcium (Ca^{2+}), Mg^{2+}, Al^{3+}, and total dissolved Fe and Mn were measured by a Perkin Elmer Model 400 inductively coupled plasma - atomic emission spectrophotometer (ICP-AES). Sodium (Na^+), K^+, and Si^{4+} were measured by a Perkin Elmer Model 500 atomic adsorption spectrophotometer (AAS). Ferrous iron (Fe^{2+}) was determined by the phenanthroline method (APHA 1992). Ferric iron (Fe^{3+}) was measured by subtraction of Fe^{2+} from Fe_{tot}. Sulfate and Cl^- were determined by Varian Model high performance liquid chromatography (HPLC). X-ray diffraction (Phillips PW 1800 diffractometer) was used to determine minerals and X-ray fluorescence (Phillips PW 1480 wavelength spectrometer) was used to determine elements on selected sediment samples.

Geochemical speciation was completed by using WATEQ4F (Ball et al. 1987). In order to implement this model, it is assumed that water conditions are at equilibrium with respect to chemical reactions. The thermodynamic data used by WATEQ4F are indicated in Table 1.

Results

The association between distance along the flow path and contact time is necessary to understand the results. Distance along the flow path corresponds to water-limestone contact time because of the consistent pumping rate (Table 2). Therefore, distance represents the length of the limestone dissolution reaction. Experimental time is the length of time since the experiment began (at the start of pumping). For instance, after two hours of pumping, water samples were taken from all ports along the flow path and the water sample from each port had a different contact time or distance at that 2 hour sampling time. For the purposes of decreasing confusion, "distance" represents contact time and "time" represents time passage since the beginning of the experiment. Figures herein show distance as the independent variable. Time since the experiment began (experimental time) is shown by data points and lines on the graphs. When all the runs were compared, the trends for each duplicate run were very similar. Therefore, representative data and figures are shown to illustrate the results.

Experiments without Sulfate

The [Fe^{3+}] decreased along the flow path, with the greatest decline in the first 23 cm (Fig. 4a). The last three quarters of the column showed further Fe^{3+} removal but not at the rate achieved in the first 23 cm. At 6 hrs after the experiment began, [Fe^{3+}] was completely removed by the effluent. At 10 and 12 hrs, the effluent [Fe^{3+}] was similar to [Fe^{3+}] at ports 2 and 3. The greatest increase in pH along the flow path occurred in the first 23 cm (Fig. 4b, remember the log nature of pH). The greatest [Ca^{2+}] increase took place in the first 23 cm (Fig. 4c), with a gradual increase in the latter 69 cm. Over

experimental time, slightly more Ca^{2+} was generated at the 6 hr sampling time than at the 12 hr sampling time. This result shows that over time the limestone either dissolved at a slower rate thereby generating less Ca^{2+} or Ca^{2+} was removed from solution by some precipitating species. This pattern of Ca^{2+} increase occurred constantly throughout the experiments.

The $[Al^{3+}]$ decreased over the length of the column (Fig. 5a) at all sampling times. The largest decrease occurred in the initial 23 cm, after which lesser amounts of Al^{3+} were removed. The $[Al^{3+}]$ was removed at greater amounts early in the experiment (6 hrs) compared to later. Water pH rose continually throughout the distance of the reactor (Fig 5b) and was greatest at earlier sampling times. The greatest pH rise was in the first 23 cm of the ALD, and $[Ca^{2+}]$ followed the same pattern over the entire run (Fig 5c). The greatest amount of Ca^{2+} was generated in the initial 23 cm, followed by lesser amounts for the remainder of the ALD. Again, the 6-hr sampling time showed greater $[Ca^{2+}]$ in the water than at 12 hrs.

The saturation index of $Fe(OH)_{3(s)}$ and the saturation index of calcite produced similar patterns (Fig. 6). There was a continual increase in saturation index for both compounds over the entire length of the flow path. After the experiment had run for 6 hrs, the saturation index remained relatively constant after the first 23 cm of the flow path. The solution was near equilibrium (10^{-1} to 10^{1}) with respect to $Fe(OH)_{3(s)}$, but the solution was highly undersaturated with respect to calcite (10^{-8}). Plots of the saturation index for $Al(OH)_{3(s)}$ and calcite exhibit the same trend, increasing with distance from the influent (Fig. 7). The largest rise occurred in the first 23 cm of the flow path, while the least rise took place in the 23 to 46 cm of the flow path. The solution remained near equilibrium with respect to $Al(OH)_{3(s)}$, while the solution remained highly undersaturated with respect to calcite.

Experiments with Sulfate

The $[Fe^{3+}]$, pH, and $[Ca^{2+}]$ changed most in the first 23 cm of the flow path (Fig. 8). The $[Fe^{3+}]$ declined rapidly in the ALD, exhibiting an opposite pattern of $[Ca^{2+}]$ (Fig. 8a and 8c). There were only minor changes in $[Fe^{3+}]$ and $[Ca^{2+}]$ later in the flow path. Water pH rose rapidly within two intervals: 0 to 23 cm and 46 to 69 cm (Fig. 8b); and sulfate declined slightly once the AMD entered the ALD (Fig. 8d).

The $[Al^{3+}]$ declined most abruptly (especially at the 2-hr sampling time) in the first 23 cm of the reactor (Fig. 9a), with a more gradual decline over the remainder of the flow path. The rate of decline slowed as the experiment progressed with an almost constant decline along the flow path at the 12-hr sampling time. The increase of pH and $[Ca^{2+}]$ showed the same trend as the decrease of $[Al^{3+}]$ (Fig. 9b and 9c). Sulfate decreased throughout the reactor at the 2-hr sampling time, but fluctuated along the flow path as the experiment continued (Fig. 9d). Water samples at 6 and 8 hrs showed an increase in sulfate in the last three quarters of the ALD, while the 12-hr samples showed a decrease in sulfate throughout the reactor. The saturation index for $Fe(OH)_{3(s)}$ increased with distance (Fig. 10a), similar to pH (Fig. 8b); and was oversaturated in the latter 46 cm of the reactor.

The saturation index increased most between 46 and 69 cm. The saturation index of calcite increased dramatically in the first 23 cm of the ALD (Fig. 10b), but stabilized over the last quarter of the flow path. The rate of increase declined over experimental time. The solution was again highly undersaturated with respect to calcite (10^{-12} to 10^{-4}).

Based on geochemical modeling, the water was oversaturated with respect to other mineral phases at various locations in the reactor and at different times during the experiment. For Fe^{3+} experiments, solutions were 3 to 5 orders of magnitude oversaturated with respect to goethite for all sampling points. Water conditions were oversaturated with respect to K-jarosite ($KFe_3(SO_4)_2(OH)_6$) at all times, whenever measurable K^+ was present. The solution remained oversaturated with respect to Na and H-jarosite ($NaFe_3(SO_4)_2(OH)_6$ and $HFe_3(SO_4)_2(OH)_6$) in the pH range 2.7 to 3.3. When pH versus $Fe(OH)_{3(s)}$ and H-jarosite saturation index are plotted for all samples containing sulfate (Fig. 11), the solution was not oversaturated with respect to any mineral phase from pH 3.1 to 4.6, although the water was nearly at equilibrium with respect to $Fe(OH)_{3(s)}$. The solution remained undersaturated with respect to gypsum for every sample.

Waters were close to equilibrium with respect to $Al(OH)_{3(s)}$ and jurbanite ($AlOHSO_4$) throughout the Al^{3+} runs (Fig. 12). The saturation index for $Al(OH)_{3(s)}$ rose as pH increased along the flow path (Fig. 12a), while the saturation index for jurbanite decreased (Fig. 12b). The saturation index for calcite resembles that of $Al(OH)_{3(s)}$ (Fig. 12c), except that the solution was highly undersaturated with respect to calcite at all times. At pH >5.1, the solution was oversaturated with respect to $Al(OH)_{3(s)}$, while at pH <5.1, the solution was oversaturated with respect to jurbanite (Fig. 13). The

solution was oversaturated with respect to gibbsite ($Al(OH)_{3(c)}$) and basaluminite ($Al_4(OH)_{10}SO_4$) at the same times as $Al(OH)_{3(a)}$. When K^+ was measurable, the solution was oversaturated with respect to alunite ($KAl_3(SO_4)_2(OH)_6$) at all pH values. The solution remained undersaturated with respect to gypsum throughout the runs.

Discussion

The changes in concentration of reacting species suggest that relative rates of dissolution and precipitation declined along the flow path and were most rapid in the first 23 cm of the reactor. The final 69 cm of the reactor produced a smaller change of concentrations at three times the flow distance. The fast initial rate in the first 23 cm is related to the low water pH, low $[Ca^{2+}]$ and high $[Me^{3+}]$. Dissolution and precipitation slowed greatly beyond 23 cm as the rates of $[Ca^{2+}]$ increase and $[Me^{3+}]$ decrease leveled off. However, calcite dissolution and metals precipitation did not fully stop, as $[Ca^{2+}]$ further increased and $[Me^{3+}]$ decreased along the reactor, albeit at a slower rate of increase than in the first 23 cm.

Dissolution and precipitation rates appeared to peak at 2 hrs, then slowed as the experiment continued up to 12 hrs. This is evident by the decrease in $[Ca^{2+}]$ and increase in $[Me^{3+}]$ with time at the same sampling points, despite uniform influent chemistry. The decrease in limestone dissolution rate is ascribed to coating of limestone surfaces with metal precipitates over time.

Precipitation of $Fe(OH)_{3(a)}$ appeared to be the controlling precipitation phase because it was nearest equilibrium, agreeing with the precipitation sequence set forth by Lindsay (1979):

$Fe(OH)_3$ (amorp) > γ-Fe_2O_3 (maghemite) > γ-FeOOH (lepidocrocite) > α-Fe_2O_3 (hematite) > α-FeOOH (goethite)

During the neutralization process, $Fe(OH)_{3(a)}$ precipitates first and rapidly enough that other iron oxyhydroxides are unable to form (Lindsay 1979). Lepidocrocite and goethite may precipitate during the neutralization process, but precipitation of these minerals is controlled by Fe^{2+} oxidation. Excess neutralization during the oxidation of Fe^{2+} allows goethite to form (Clarke et al. 1985). Lepidocrocite is able to form in the presence of the citrate ligand. Citrate slows Fe^{2+} oxidation, thereby allowing for slower precipitation of Fe^{3+} (Krishnamurti and Huang 1993). Since very little Fe^{2+} was present, lepidocrocite and goethite precipitation were unlikely.

The Al^{3+} experiments appeared to be controlled by $Al(OH)_{3(a)}$ because of its nearness to equilibrium. Again, agreement with the precipitation of aluminum hydroxides, oxyhydroxides, and oxides is seen (Lindsay 1979):

$Al(OH)_3$ (amorp) > α-$Al(OH)_3$ (bayerite) > γ-AlOOH (boehmite) > $Al(OH)_3$ (norstrandite) > γ-$Al(OH)_3$ (gibbsite) > α-AlOOH (diaspore)

Anhydrous oxide phases such as γ-$Al_2O_{3(c)}$ and α- Al_2O_3 (corundum) are high temperature minerals and are unlikely to precipitate at low temperatures (Lindsay 1979). In addition to being the least soluble, $Al(OH)_{3(a)}$ is also the least structurally complex (Dixon and Weed 1989), indicating that $Al(OH)_{3(a)}$ formation should take place first, thus controlling precipitation. The solution was highly oversaturated with respect to diaspore and boehmite. Because these minerals are more structurally complex and require longer time periods to form, they may be kinetically inhibited. Precipitation was probably kinetically much faster for $Al(OH)_{3(a)}$ such that other Al^{3+} precipitation phases would not form.

The saturation index plots appeared to follow pH for the respective experiments (Figs. 9b, 10b, 11b, and 12b) in both distance and sampling time, indicating that pH is controlling solid phase formation. This should be true because Me^{3+} hydrolysis is pH dependent (Stumm and Morgan 1996). The highest saturation index for $Fe(OH)_{3(a)}$, $Al(OH)_{3(a)}$, and calcite occurred when pH and $[Ca^{2+}]$ was high and $[Me^{3+}]$ was low. As pH decreased, the $Me(OH)_3$ saturation index moved closer to equilibrium, meaning that the reactor may be moving toward a stable state.

When sulfate was added, Fe^{3+} experiments show that the solution became oversaturated with respect to jarosite minerals. However, these minerals probably did not form because jarosite mineral formation takes days or weeks to occur whenever the solution was highly conducive to jarosite formation (Ivarson et al. 1982, Stahl et al. 1993). Additionally, there is evidence to suggest that jarosite forms from $Fe(OH)_{3(a)}$ during aging in the presence of the proper cations (Lindsay 1979).

When sulfate was added in Al^{3+} experiments, the possibility existed that other minerals controlled the precipitation of aluminous compounds. The solution was oversaturated with respect to jurbanite at pH <5.1 (Fig. 13). When pH was <5.1, most of the Al^{3+} was lost, indicating that the quantity of jurbanite that precipitated would be much greater than $Al(OH)_{3(a)}$. Stoichiometrically, this does not fit our results. Because

the Al^{3+} to sulfate ratio of jurbanite is 1/1, the loss of 1 mmol of Al^{3+} should correspond to the loss of 1 mmol of sulfate if jurbanite was the controlling precipitation phase. Approximately 4 mmol of Al^{3+} precipitated and <1 mmol of sulfate were removed in our experimental solutions when the pH <5.1, suggesting that a phase other than jurbanite was controlling Al^{3+} precipitation. Additionally, XRD data did not detect large amounts of sulfate mineral precipitation. Gibbsite is not likely to precipitate because the more soluble $Al(OH)_{3(a)}$ precipitates more rapidly during pH rise (Lindsay 1979). Alunite must have precipitated in minimal amounts because very little potassium was available. Basaluminite was most likely kinetically inhibited, consistent with other studies (Nordstrom 1982).

The saturation index of calcite did not stabilize such as that observed in experiments not containing sulfate, but the rate at which progression toward equilibrium took place did drop greatly, possibly indicating that dissolution was greater throughout the reactor when sulfate was added. It can be inferred that the reason for increased dissolution in experiments with sulfate was that the influent water was more acidic, which would allow for greater H^+ diffusion to the limestone surface.

The enhanced dissolution may also have been a result of higher ionic strength, which may have increased the solubility of the metals (Hayden and Rubin 1974, Roberson and Hem 1967, Tipping et al. 1988). As influent sulfate concentration increased, complexation of metals increased, thereby suppressing $Me(OH)_{3(a)}$ precipitation. Additionally, when particles did coagulate, sedimentation may have been more difficult. As the number of particles in a suspension increase, the sedimentation rate is hindered because water must move up through the particles as the particles settle (Tchobanoglous and Burton 1991). The combination of increases in ionic strength and number of particles in suspension allows for the increase in pH observed and the greater limestone dissolution.

The solution remained highly undersaturated with respect to calcite for the entirety of experiments. Because limestone dissolution in acidic solutions is rapid, it was expected that the solution would approach equilibrium with respect to calcite (Pearson and McDonnell 1975, duPlessis and Maree 1992). The bulk solution may not have been in equilibrium with respect to calcite because precipitation reactions may have coated limestone, inhibiting dissolution, and thereby maintaining highly undersaturated conditions in the solution. It can be speculated that calcite was near equilibrium at the limestone surface because the saturation index rose minimally in the last 69 cm of the reactor after 2 hrs. If this is the case, disequilibrium can be promoted if Ca^{2+} or inorganic carbon species can be moved from limestone surfaces or H^+ can be moved to the surface. Because movement of ions to and from limestone surfaces is diffusion controlled, a precipitation barrier appears to have limited the diffusion process, limiting dissolution, and thereby keeping the bulk solution undersaturated with respect to calcite.

Conclusions

The results of these experiments are significant to the design of an ALD in the field. If the water has DO <1 mg L^{-1} and no Fe^{3+} or Al^{3+} in the water, the limestone dissolution should continue unabated, increasing the pH to around 6.0 and increasing alkalinity in the water. Upon exiting the ALD, the water will oxidize, metal hydroxides will form due to excess bicarbonate alkalinity and will precipitate in settling ponds. An ALD is not recommended for waters containing greater than 25 mg L^{-1} of Fe^{3+} or Al^{3+}.

In water containing small amounts of Fe^{3+} or Al^{3+} (as is almost always the case in the field), an ALD may still be used. It is apparent that ALDs serve as sinks for Fe^{3+} and Al^{3+} hydroxide precipitation. The formation and precipitation of these minerals in an ALD is rapid and require less than 1 hr for the majority of the mineral phases to form and precipitate. Field ALDs fail when water does not flow out at the effluent pipe and water exits before reaching the end of the ALD due to reduced permeability caused by metal hydroxides plugging the flow path. In a large ALD, much of the limestone later in the flow path remains unreacted because the majority of dissolution occurred at the front of the ALD, raising pH, thereby leaving little acidity to cause limestone dissolution later in the system.

The implications of this research suggest that ALDs could be built smaller than those currently being constructed in the field. Water-limestone contact times may need to be only 1 to 2 hrs to neutralize metals to an appreciable level rather than the 15 to 20 hrs contact time presently recommended (Hedin et al. 1994). As the pore space in the limestone is occluded by metal hydroxides, the ALD can be replaced. Under these conditions, less limestone is wasted, smaller spatial requirements are needed for installation of the ALD, and replacement of a smaller ALD on a more frequent interval may be less expensive.

Literature Cited

American Public Health Association, American Water Works Association, Water Environment Federation. A. E. Greenberg (ed). 1992. Standard methods for the examination of water and wastewater. 18th ed. Washington, D.C.

Ball, J.W., E.A. Jenne, and D.K. Nordstrom. 1979. WATEQ2-A computerized chemical model for trace and major elemental speciation and mineral equilibria of natural waters. p. 815-836. *In*: E.A. Jenne (ed.), Chemical Modeling in Aqueous Systems. American Chemical Society Symposium Series 93, U.S. Govt. Printing Office, Washington, DC.

Ball, J. W., D. K. Nordstrom, and D. W. Zuckmann. 1987. WATEQ4F- a personal computer translation of the geochemical model WATEQ2 with revised database. Open file report. U. S. Geological Survey 87-50. U.S. Govt. Printing Office, Washington, DC.

Clarke, E. T., R. H. Loeppert, and J. M. Ehrman. 1985. Crystallization of iron oxides on calcite surfaces in static systems. Clays and Clay Minerals. 33:152-158.
https://doi.org/10.1346/CCMN.1985.0330210

Dixon, J. B. and S. B. Weed. 1989. Minerals in soil environments. 2nd ed. Soil Science Society of America. Madison, WI.

du Plessis, P. and J. P. Maree. 1992. Neutralization of acid water in the chemical industry with limestone. Water Science and Technology. 29(8): 93-104.

Hayden, P. L. and A. J. Rubin. 1974. Systematic investigation of the hydrolysis and precipitation of aluminum(III). *In* A. J. Rubin (ed). Aqueous-Environmental Chemistry of Metals. Ann Arbor Science. Ann Arbor, MI.

Hedin, R. S. and G. R. Watzlaf. 1994. The effects of anoxic limestone drains on mine water chemistry. p. 185-194. *In:* Proceedings, International Land Reclamation and Mine Drainage Conference and 3rd International Conference on the Abatement of Acidic Drainage. Pittsburgh, PA, April 24-27, 1994.
https://doi.org/10.21000/JASMR94010185

Hedin, R. S., G. R. Watzlaf, and R. W. Nairn. 1994. Passive treatment of acid mine drainage with limestone. Journal of Environ. Quality 13: 1338-1345.
https://doi.org/10.2134/jeq1994.00472425002300060030x

Ivarson, K. C., G. J. Ross, and N. M. Miles. 1982. Mineralogical transformations of iron and sulfate soils and tidal marshes. *In:* Kittrick, J. A., D. S. Fanning, and L. R. Hossner (eds.), Acid Sulfate Weathering. Soil Science Society of America Special Publication #10. Soil Science Society of America. Madison, WI.

Krishnamurti, G. S. R. And P. M. Huang. 1993. Formation of lepidocrocite from iron(II) solutions: stabilization by citrate. Soil Science Society of America Journal. 57: 861-867.
Apparently there is an error in this citation.

Langmuir, D. 1969. The Gibbs free energies of substances in the system Fe-O_2-H_2O-CO_2 at 25°C. p. B180-B183. *In*: Geological Survey Research 1969. U.S. Geological Survey Professional Paper 650-B. U.S. Govt. Printing Office, Washington, DC.

Lindsay, W. L. 1979. Chemical equilibria in soils. 1st ed. John Wiley and Sons. New York, NY.

Nordstrom, D. K. 1982. Aqueous pyrite oxidation and the consequent formation of secondary minerals. p. 37-56. *In:* Kittrick, J. A., D. S. Fanning, and L. R. Hossner (eds.), Acid Sulfate Weathering. Soil Science Society of America special publication #10. Soil Science Society of America. Madison, WI.

Nordstrom, D.K., L.N. Plummer, D. Langmuir, E. Busenberg, H.M. May, B.F. Jones, and D.L. Parkhurst. 1990. Revised chemical equilibrium data for major water mineral reactions and their limitations. p. 398-413. *In*: D.C. Melchor and R.L. Bassett (eds.), Chemical Modeling in Aqueous Systems. American Chemical Society Symposinm Series, Washington, DC.

Pearson, F. H. and A. J. McDonnell. 1975. Use of crushed limestone to neutralize acid wastes. Journal of the Environmental Engineering Division, ASCE. No. FE1 Proc. Paper 11131. 101: 138-158.

Plummer, L.N., and E. Busenberg. 1982. The solubilities of calcite, aragonite and vaterite in CO_2 solutions between 0 and 90°C, and an

evaluation of the aqueous model for the system $CaCO_3$-CO_2-H_2O. Geochemica et Cosmochimica Acta. 46: 1011-1040.
https://doi.org/10.1016/0016-7037(82)90056-4

Rawajfih, Z. 1975. The solubilities of aluminum-hydroxy-sulfate compounds as a possible mechanism of sulfate retention by soils. Ph.D. Dissertation, Auburn University, Auburn, AL.

Roberson, C. E. and J. D. Hem. 1967. Solubility of aluminum in the presence of hydroxide, fluoride and sulfate. United States Geologic Survey Water Supply Paper 1827-C. U.S. Govt. Printing Office, Washington, DC.

Robie, R.A., and D.R. Waldbaum. 1968. Thermodynamic properties of minerals and related substances at 298.15 K and one atmosphere pressure and at higher temperatures. U.S. Geological Survey Bulletin 1259, U.S. Govt. Printing Office, Washington, DC.

Singh, S.S. 1969. Basic aluminum sulfate formed as a metastable phase and its transformation to gibbsite. Canadian Journal of Soil Science 49: 383-388.
https://doi.org/10.4141/cjss69-052

Skousen, J. G. 1991. Anoxic limestone drains for acid mine drainage treatment. Green Lands 21(4): 30-35.

Skousen, J., A. Sexstone, K. Garbutt, and J. Sencindiver. 1992. Wetlands for treating acid mine drainage. Green Lands 22(4): 31-39.

Stahl, R. S., D. S. Fanning, and B. R. James. 1993. Goethite and jarosite precipitation from ferrous sulfate solutions. Soil Science Society of America Journal 57: 280-282.
https://doi.org/10.2136/sssaj1993.03615995005700010047x

Stumm, W. and J. J. Morgan. 1996. Aquatic chemistry: an introduction emphasizing chemical equilibria in natural waters. 3rd ed. John Wiley and Sons. New York, NY.

Tchobanoglous, G. and F. Burton. 1991. Wastewater engineering- treatment, disposal, and reuse. 3rd ed. McGraw-Hill, Inc. New York, NY.

Tipping, E., C. Woof, P. B. Walters, and M. Ohnstad. 1988. Conditions required for the precipitation of aluminum an acidic natural waters. Water Research 22(5): 585-592.
https://doi.org/10.1016/0043-1354(88)90059-0

Turner, D. and D. McCoy. 1990. Anoxic alkaline drain treatment system, a low cost acid mine drainage treatment alternative. *In:* D. H. Graves (ed.), Proceedings, National Symposium on Mining, Lexington, KY. May 14-18, 1990. University of Kentucky, Lexington , KY.

Wagman, D.D., W.H. Evans, V.B. Parker, I. Halow, S.M. Bailey, and R.H. Schumm. 1968. Selected values of chemical thermodynamic properties. Tables for the first thirty-four elements in the standard order of arrangement. National Bureau of Standards Technical Note 270-3. U.S. Govt. Printing Office, Washington, DC.

Table 1. Table of solubility products at 298.15 K.

Species	Reaction	Log K_{sp}	Reference
Ferrihydrite*	$Fe(OH)_3 + 3\ H^+ \leftrightarrow Fe^{3+} + 3\ H_2O$	9.66	Langmuir (1969)
Goethite	$FeOOH + 3\ H^+ \leftrightarrow Fe^{3+} + 2\ H_2O$	-1.0	Nordstrom et al. (1990)
Jarosite-Na	$NaFe_3(SO_4)_2(OH)_6 + 6\ H^+ \leftrightarrow Na^+ + 3\ Fe^{3+} + 2\ SO_4^{2-} + 6\ H_2O$	-11.2	Ball et al. (1979)
Jarosite-K	$KFe_3(SO_4)_2(OH)_6 + 6\ H^+ \leftrightarrow K^+ + 3\ Fe^{3+} + 2\ SO_4^{2-} + 6\ H_2O$	-14.8	Ball et al. (1979)
Jarosite-H	$(H_3O)Fe_3(SO_4)_2(OH)_6 + 6\ H^+ \leftrightarrow H_3O^+ + 3\ Fe^{3+} + 2\ SO_4^{2-} + 6\ H_2O$	-5.39	Ball et al. (1979)
$Al(OH)_{3(a)}$	$Al(OH)_3 + 3\ H^+ \leftrightarrow Al^{3+} + 3\ H_2O$	9.66	Lindsay (1979)
Gibbsite	$Al(OH)_3 + 3H^+ \leftrightarrow Al^{3+} + 3\ H_2O$	8.11	Nordstrom et al. (1990)
Boehmite	$AlOOH + 3\ H^+ \leftrightarrow Al^{3+} + 2\ H_2O$	8.584	Robie and Waldbaum (1968)
Diaspore	$AlOOH + 3\ H^+ \leftrightarrow Al^{3+} + 2\ H_2O$	6.879	Wagman et al. (1968)
Jurbanite	$AlOHSO_4 + H^+ \leftrightarrow Al^{3+} + SO_4^{2-} + H_2O$	-3.23	Rawajfih (1975)
Basaluminite	$Al_4(OH)_{10}SO_4 + 10\ H^+ \leftrightarrow 4\ Al^{3+} + SO_4^{2-} + 10\ H_2O$	22.7	Singh (1969)
Alunite	$KAl_3(SO_4)_2(OH)_6 \leftrightarrow K^+ + 3\ Al^{3+} + 2\ SO_4^{2-} + 6\ H_2O$	-1.4	Nordstrom et al. (1990)
Gypsum	$CaSO_4 \bullet 2\ H_2O \leftrightarrow Ca^{2+} + SO_4^{2-} + 2\ H_2O$	-4.58	Nordstrom et al., (1990)
Calcite	$CaCO_3 \leftrightarrow Ca^{2+} + CO_3^{2-}$	-8.48	Plummer and Busenberg (1982)
pK_{CO_2}	$CO_2 + H_2O \leftrightarrow H_2CO_3^*$	1.47	Plummer and Busenberg (1982)
pK_1	$H_2CO_3 \leftrightarrow HCO_3^- + H^+$	6.35	Plummer and Busenberg (1982)
pK_2	$HCO_3^- \leftrightarrow CO_3^{2-} + H^+$	10.33	Plummer and Busenberg (1982)

* Ferrihydrite will be referred to as $Fe(OH)_{3(a)}$, as this is a more appropriate description.

Table 2. Relationship between flow distance and water-limestone contact time.

Port	Distance (cm)	Contact Time (hr)
Inf	0.0	0.0
1	22.9	1.2
2	45.7	2.4
3	68.6	3.6
4	91.4	4.8

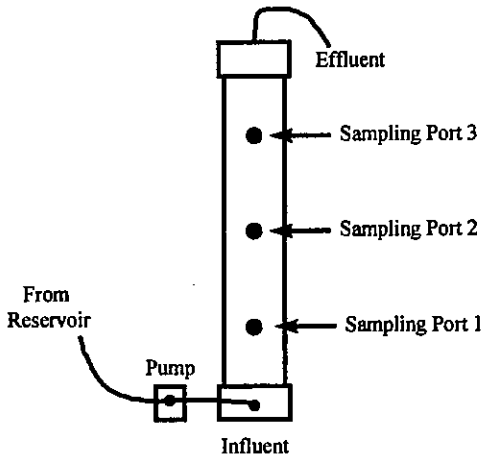

Figure 1. Depiction of laboratory anoxic limestone drain.

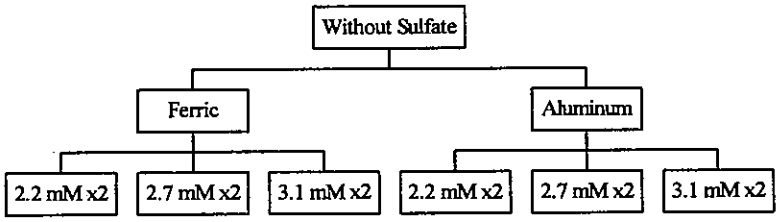

Figure 2. Module 1- Experiments without sulfate.

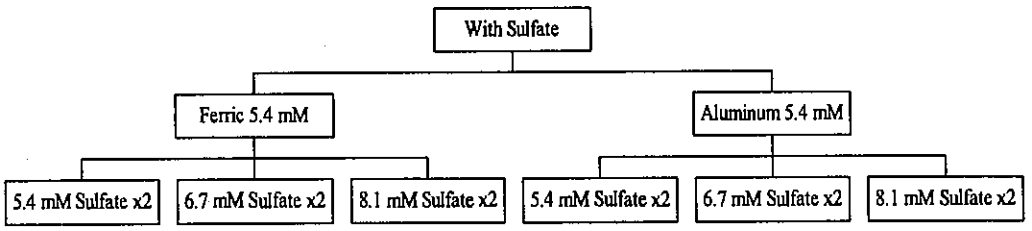

Figure 3. Module 2- Experiments with sulfate.

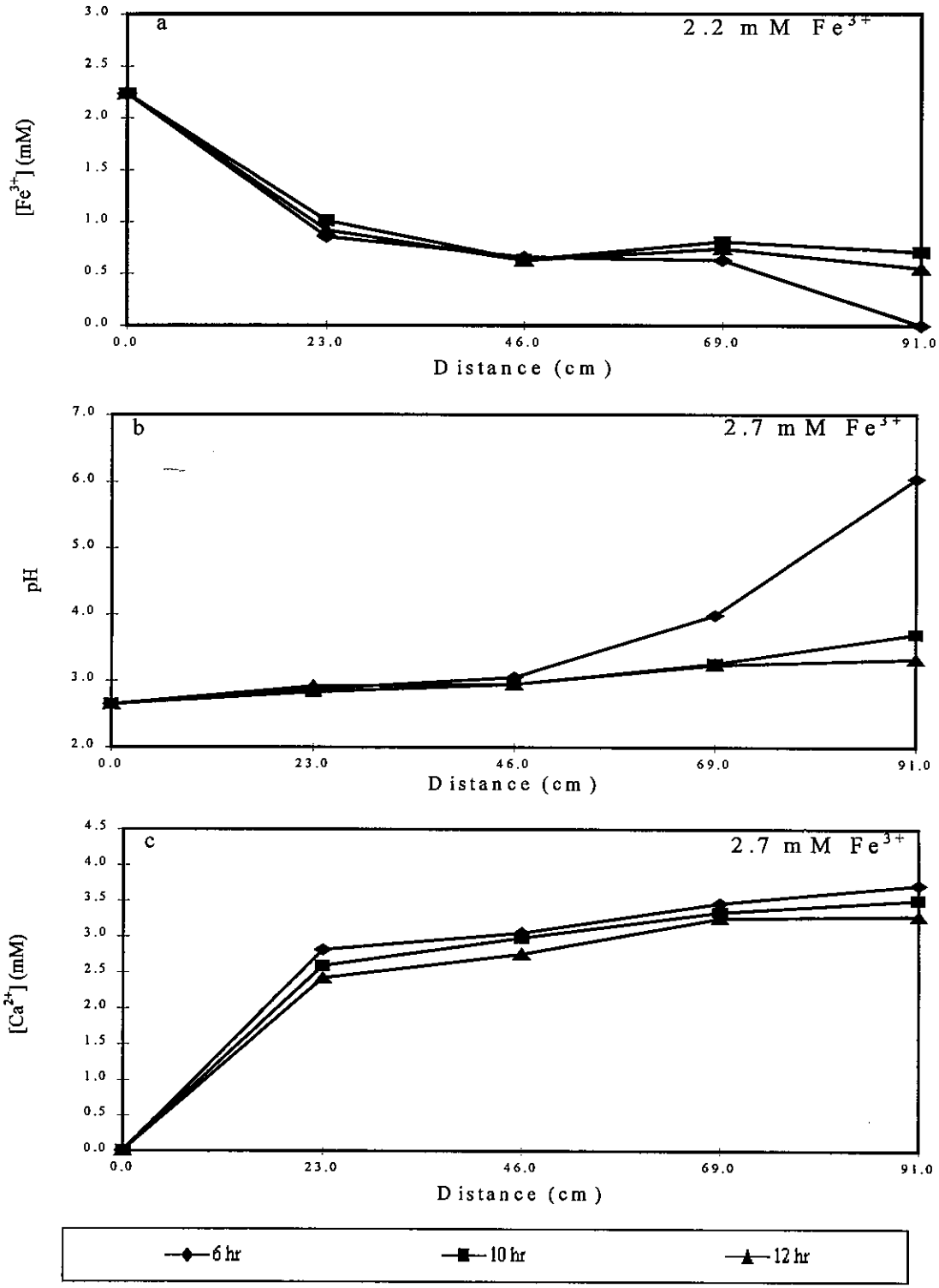

Figure 4. Concentration versus distance for Fe^{3+} runs without sulfate. Responses of ions in solution: Fe^{3+} (a), pH (b), and Ca^{2+} (c).

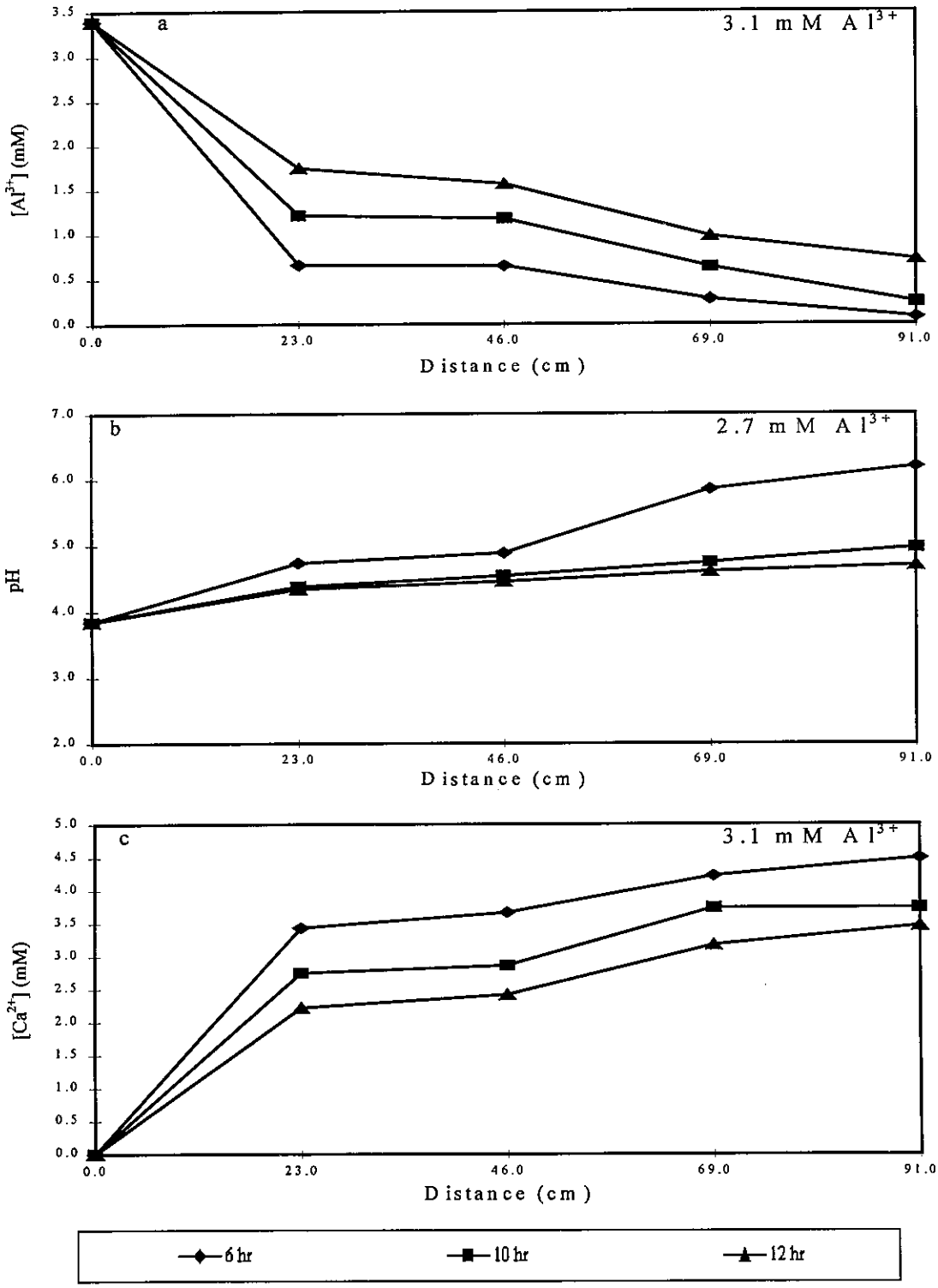

Figure 5. Concentration versus distance for Al^{3+} runs without sulfate. Responses of ions in solution: Al^{3+} (a), pH (b), and Ca^{2+} (c).

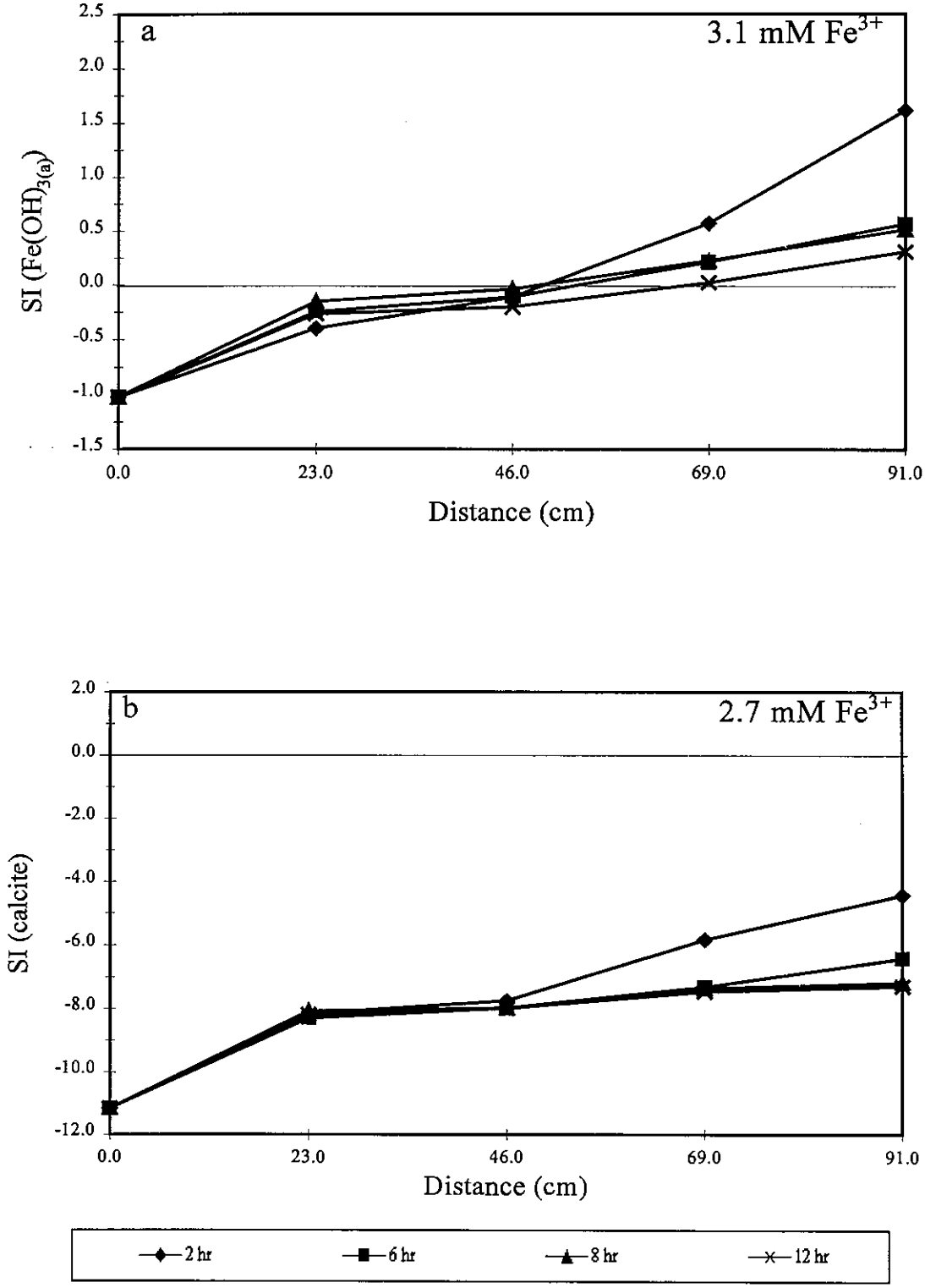

Figure 6. Saturation index (SI) versus distance for Fe^{3+} experiments without sulfate. Responses of SI: $Fe(OH)_{3(a)}$ (a) and calcite (b).

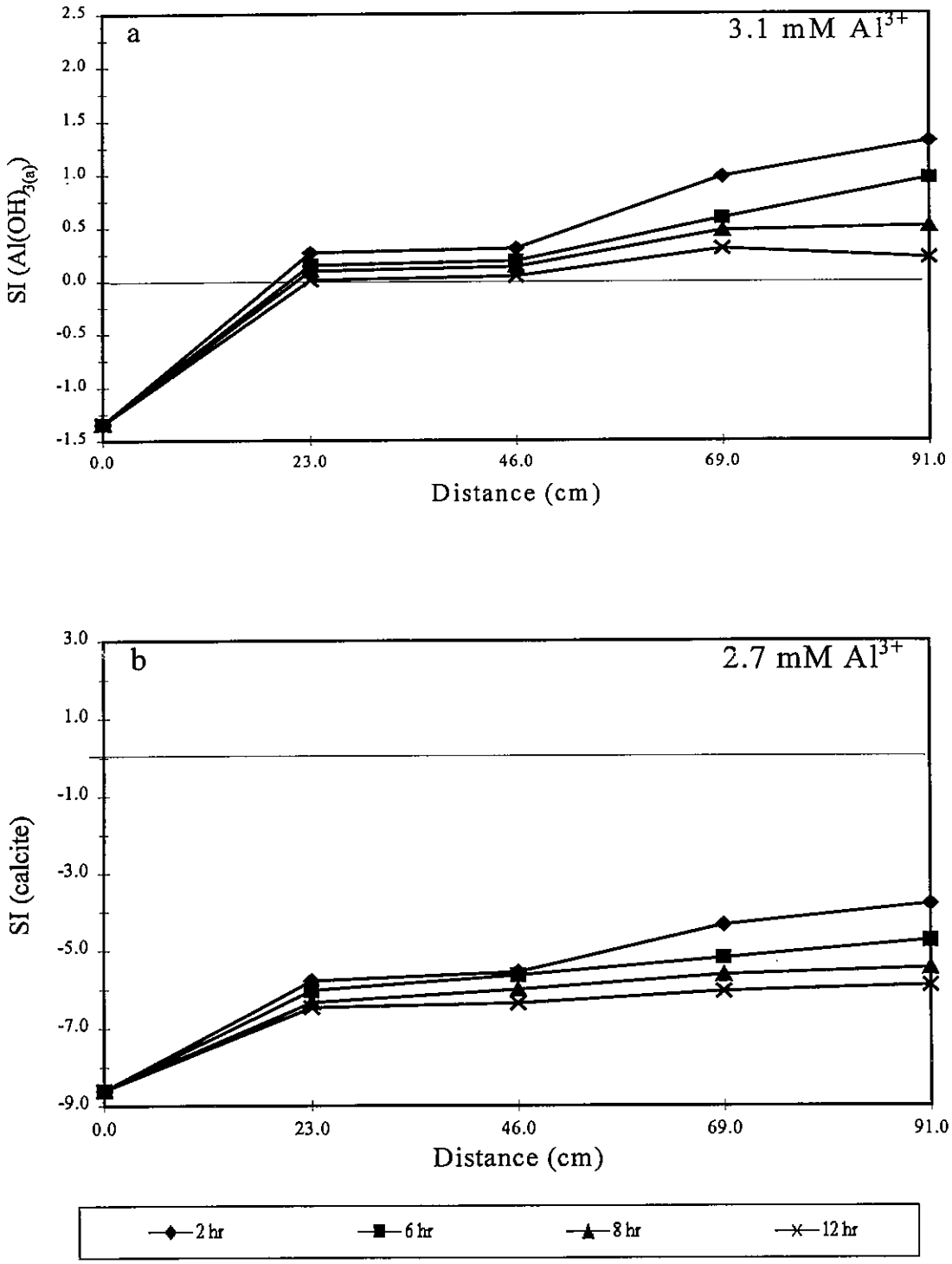

Figure 7. Saturation index (SI) versus distance for Al^{3+} experiments without sulfate. Responses of SI: $Fe(OH)_{3(a)}$ (a) and calcite (b).

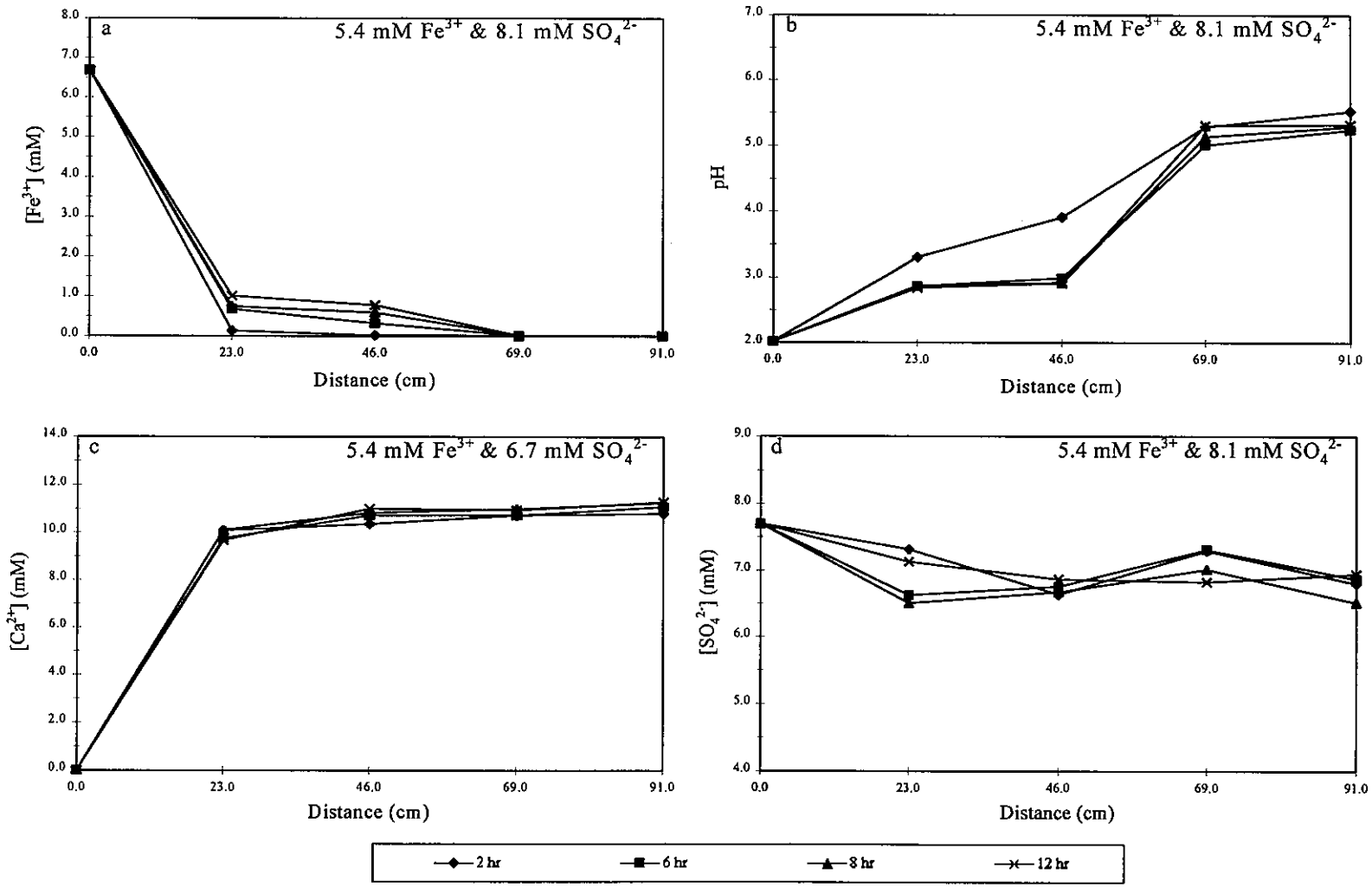

Figure 8. Concentration versus distance for Fe^{3+} runs with sulfate. Responses of ions in solution: Fe^{3+} (a), pH (b), Ca^{2+} (c), and SO_4^{2-} (d).

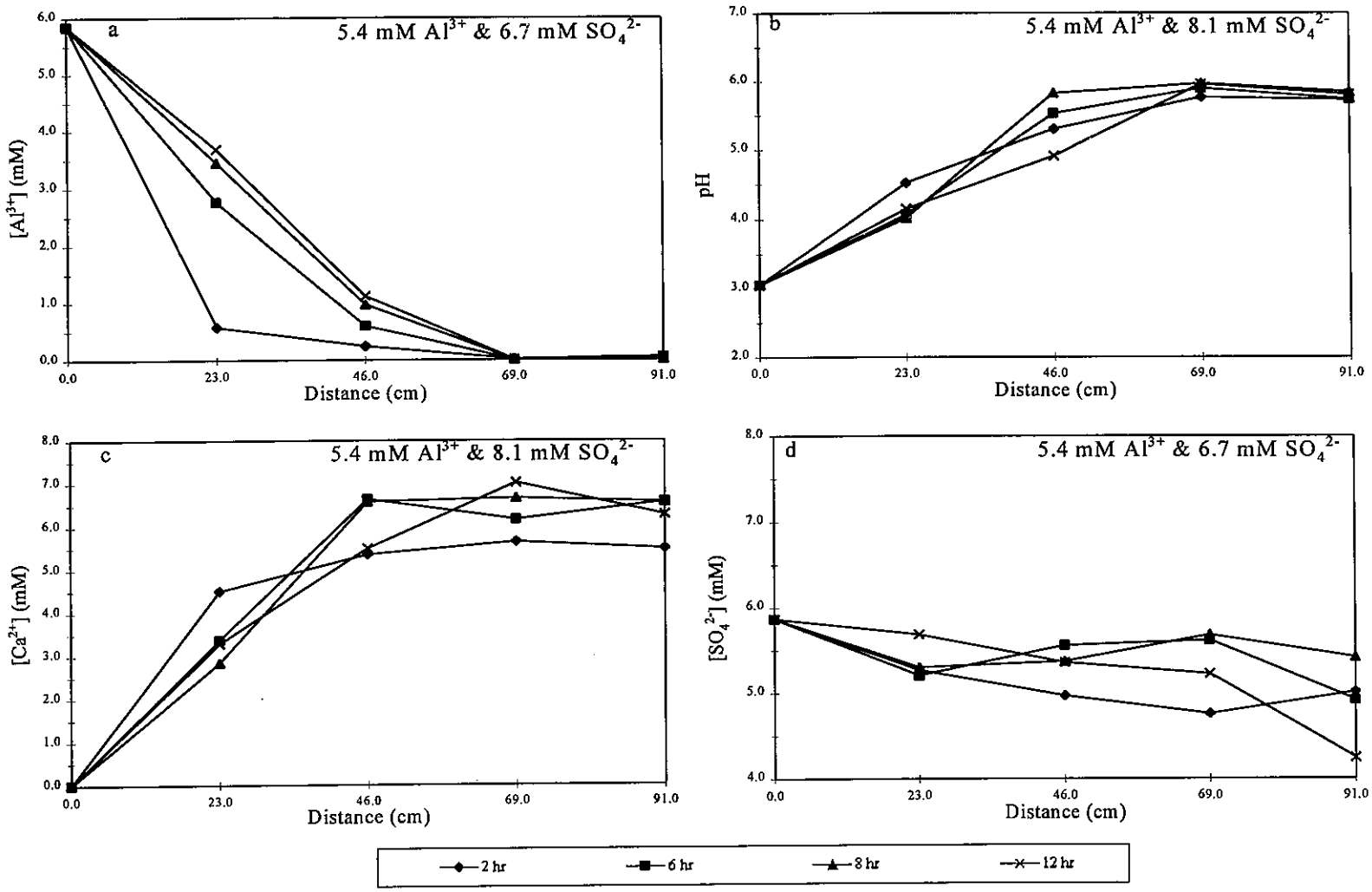

Figure 9. Concentration versus distance for Al^{3+} runs with sulfate. Responses in solution: Al^{3+} (a), pH (b), Ca^{2+} (c), and SO_4^{2-} (d).

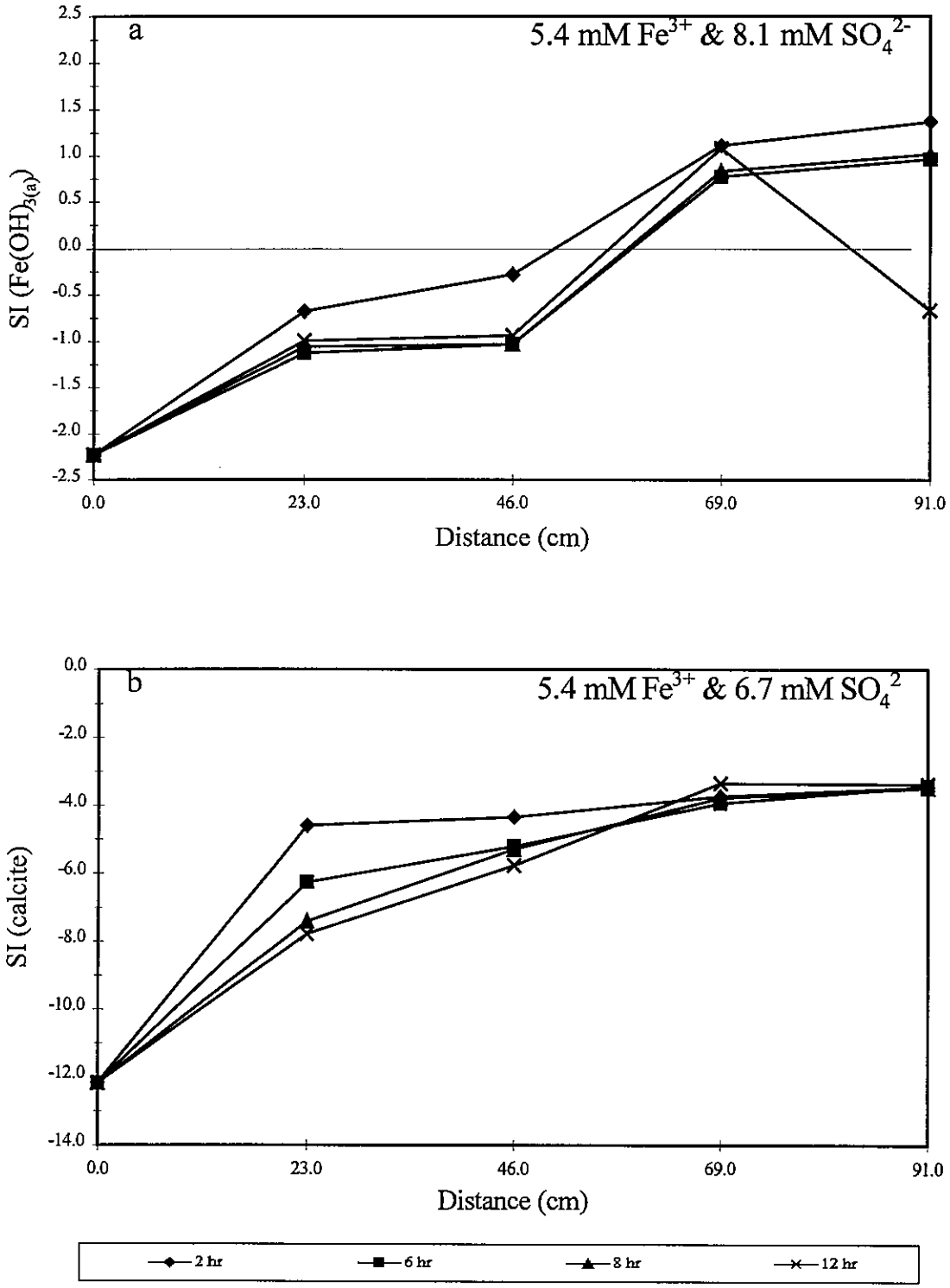

Figure 10. Saturation index (SI) versus distance for Fe^{3+} experiments with sulfate. Responses of SI: $Fe(OH)_{3(a)}$ (a) and calcite (b).

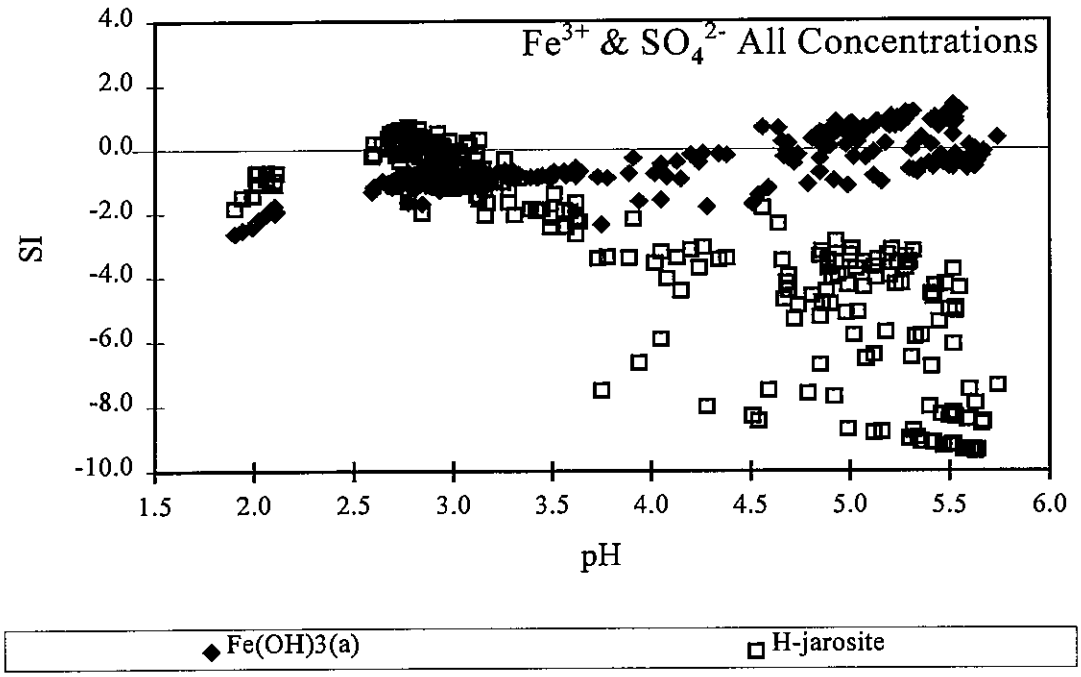

Figure 11. pH versus $Fe(OH)_{3(a)}$ and H-jarosite showing gap in oversaturated mineral phase between pH = 3.1 and 4.6.

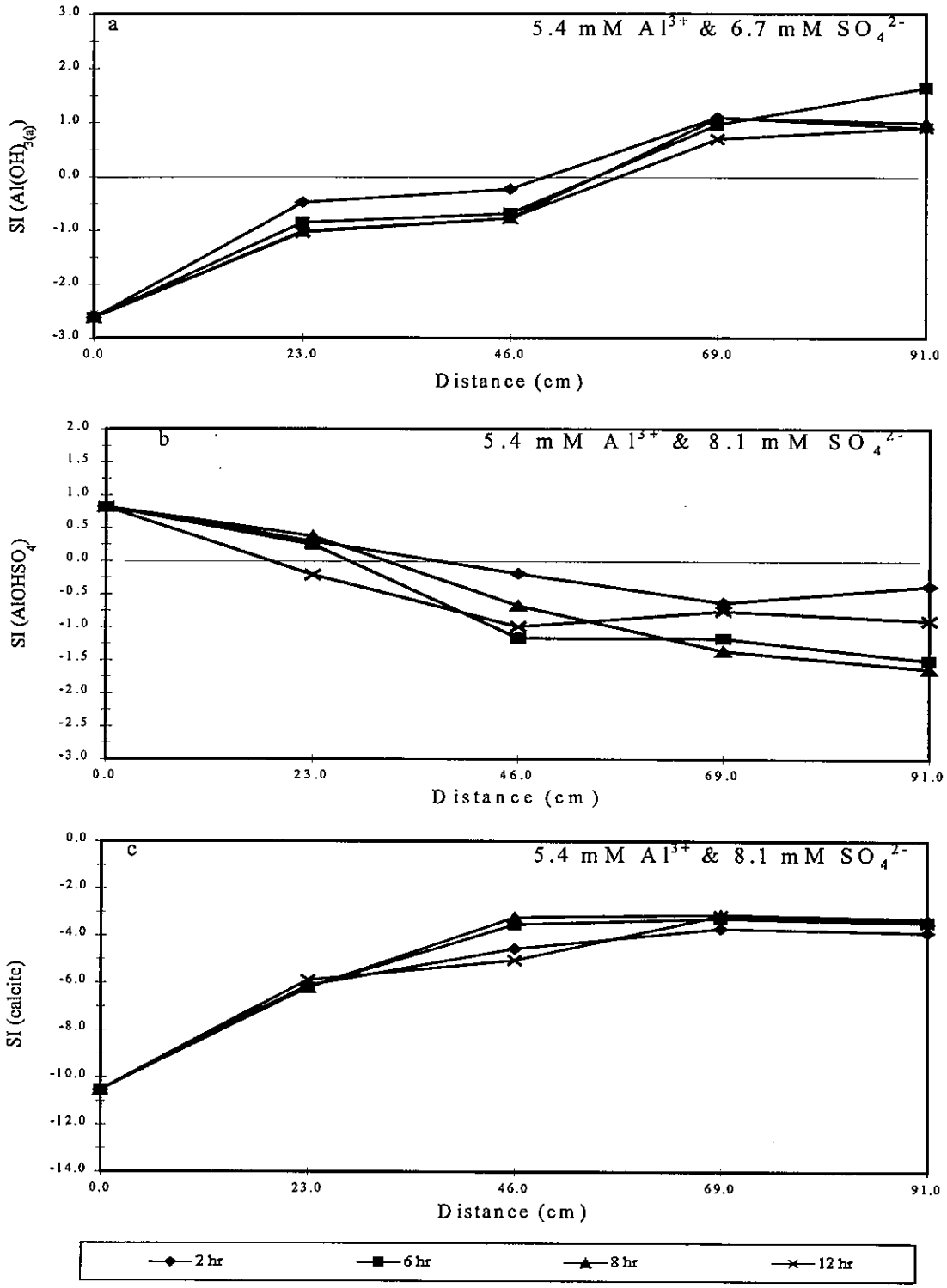

Figure 12. Saturation index (SI) versus distance for Al^{3+} experiments with sulfate. Responses for SI: $Al(OH)_{3(a)}$ (a), $AlOHSO_4$ (b), and calcite (c).

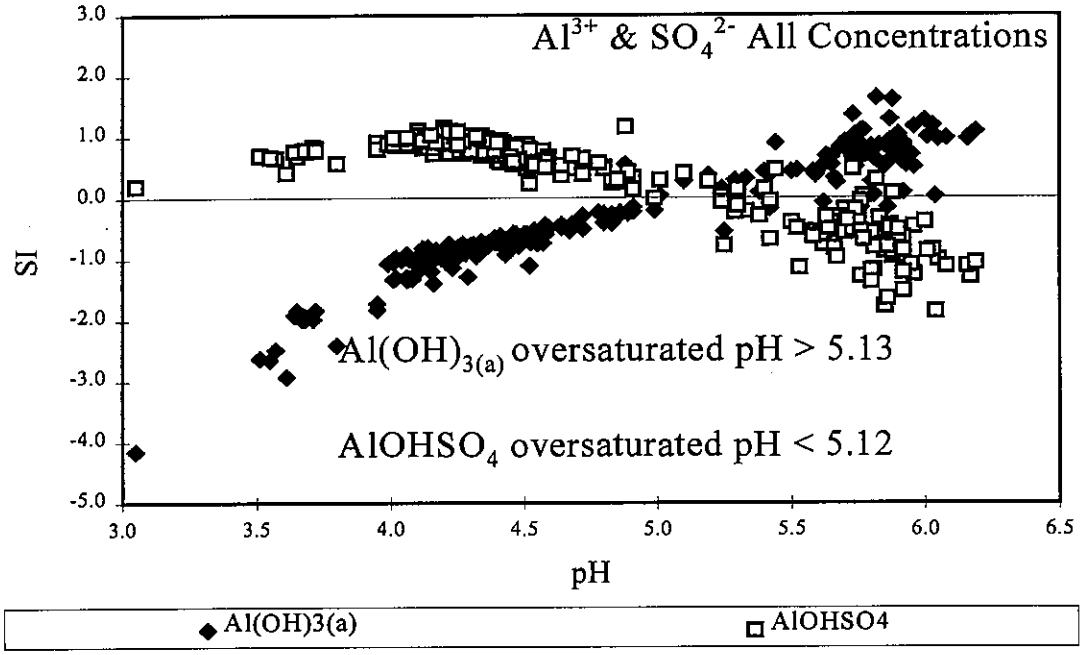

Figure 13. pH versus $Al(OH)_{3(a)}$ and jurbanite showing pH dependence of SI.